

Continuous weak measurement and feedback control of a solid-state charge qubit: physical unravelling of non-Lindblad master equation

Shi-Kuan Wang, Jinshuang Jin * and Xin-Qi Li[†]

State Key Laboratory for Superlattices and Microstructures, Institute of Semiconductors,
Chinese Academy of Sciences, P.O. Box 912, Beijing 100083, China

(Dated: October 4, 2018)

Conventional quantum trajectory theory developed in quantum optics is largely based on the physical unravelling of Lindblad-type master equation, which constitutes the theoretical basis of continuous quantum measurement and feedback control. In this work, in the context of continuous quantum measurement and feedback control of a solid-state charge qubit, we present a *physical* unravelling scheme of *non-Lindblad type* master equation. Self-consistency and numerical efficiency are well demonstrated. In particular, the control effect is manifested in the detector noise spectrum, and the effect of measurement voltage is discussed.

I. INTRODUCTION

Quantum trajectory theory has been developed and intensively applied in quantum optics [1, 2, 3, 4, 5, 6, 7]. However, the theory is largely based on unravelling of Lindblad-type master equation, which has clear physical interpretation [6]. For non-Lindblad type master equation [8], or even the non-Markovian dissipative dynamics [9, 10, 11, 12], unravelling in terms of stochastic differential equation has also been established for various purposes. Nevertheless, these schemes lack physical interpretation, having thus only mathematical meaning.

In solid-state system, the quantum measurement [13, 14, 15, 16, 17] of solid-state qubit and feedback control [18, 19, 20] have been an extensively studied subject in recent years, being largely stimulated by the prospect of solid-state quantum computing. The theoretical description of this solid-state qubit measurement problem was developed originally in terms of the “ n ”-resolved master equation [13, 14], where “ n ” stands for the number of electrons passed through the measurement apparatus. Alternatively, Bayesian formalism [15] and also the conventional quantum trajectory theory [17] were developed for this solid-state measurement setup. Being of interest, it can be shown that all these three approaches are precisely equivalent to each other.

More specifically, for the setup of a pair of coupled quantum dots (CQDs) qubit measured by a quantum point contact (QPC) detector, which has become an experimentally studied system [21], we found that the above mentioned theories were restricted to the limit of large measurement voltage across the QPC [22, 23]. At finite voltages, i.e., as the measurement voltage is comparable to or not much higher than the qubit’s intrinsic energy scale, the measurement dynamics is governed by a non-Lindblad type master equation [22]. In this regime, the “ n ”-resolved master equation was also developed to study

the readout characteristics [23]. In the present work, we further extend it to a quantum trajectory theory, which conditions the state evolution on the *entire measurement records*. It is well known that this kind of description is essential to the quantum feedback control and other possible applications.

The paper is organized as follows. In Sec. II we first present a brief description for the setup under study, then outline the “ n ”-resolved master equation for the measurement. In connection with the conditional state evolution, physical unravelling scheme is constructed and practical Monte Carlo simulation is carried out. Also, for completeness and latter use, a generalized quantum-jump approach is formulated for the calculation of noise spectrum. For the sake of brevity, some complicated expressions and mathematical details are put in two Appendices. In Sec. III we apply the developed formalism to the study of feedback control, based on a suboptimal feedback algorithm. Finally, conclusion is presented in Sec. IV.

II. CONTINUOUS MEASUREMENT OF A CHARGE QUBIT

A. Model Description

Let us consider a solid-state charge qubit measured by a nearby mesoscopic detector. In this work, as well studied in literature [13, 15, 16, 17], the charge qubit is modelled by a pair of coherently coupled quantum dots with an extra electron in it, and the mesoscopic detector can be a mesoscopic quantum point contact (QPC). The Hamiltonian of this qubit-plus-detector setup reads

$$H = H_0 + H' \quad (1a)$$

$$H_0 = H_{qb} + \sum_k (\epsilon_k^L c_k^\dagger c_k + \epsilon_k^R d_k^\dagger d_k) \quad (1b)$$

$$H_{qb} = \epsilon_a |a\rangle\langle a| + \epsilon_b |b\rangle\langle b| + \Omega(|b\rangle\langle a| + |a\rangle\langle b|) \quad (1c)$$

$$H' = \sum_{k,q} [(\mathcal{T}_{kq} + \chi_{kq} |a\rangle\langle a|) c_k^\dagger d_q + \text{H.c.}] \quad (1d)$$

*Present address: Department of Chemistry, Hong Kong University of Science and Technology, Kowloon, Hong Kong

[†]E-mail: xqli@red.semi.ac.cn

In this decomposition, the free part of the total Hamiltonian, H_0 , contains Hamiltonians of the measured qubit H_{qb} and the QPC's reservoirs. The operators $c_k^\dagger (c_k)$ and $d_k^\dagger (d_k)$ are, respectively, the electronic creation (annihilation) operators of the QPC's left and right reservoirs. The qubit states $|a\rangle$ and $|b\rangle$ correspond to the electron locating in the left and right dots. Introducing $\epsilon = (\epsilon_a - \epsilon_b)/2$ and taking $(\epsilon_a + \epsilon_b)/2$ as the reference energy, the qubit eigenenergies read $E_1 = \sqrt{\epsilon^2 + \Omega^2} = \Delta/2$, and $E_2 = -\sqrt{\epsilon^2 + \Omega^2} = -\Delta/2$. Correspondingly, the eigenstates are $|1\rangle = \cos \frac{\theta}{2}|a\rangle + \sin \frac{\theta}{2}|b\rangle$ for the excited state, and $|0\rangle = \sin \frac{\theta}{2}|a\rangle - \cos \frac{\theta}{2}|b\rangle$ for the ground state, where θ is defined by $\cos \theta = 2\epsilon/\Delta$, and $\sin \theta = 2\Omega/\Delta$.

For the sake of simplicity, we assume $\mathcal{T}_{kq} = \mathcal{T}$ and $\chi_{kq} = \chi$, i.e., the tunneling amplitudes are real and reservoir-state independent. Corresponding to the qubit states $|a\rangle$ and $|b\rangle$, the stationary detector currents read $I_a = 2\pi g_L g_R (\mathcal{T} + \chi)^2 V$, and $I_b = 2\pi g_L g_R \mathcal{T}^2 V$, respectively, where $g_{L(R)}$ is the density of state of the left (right) reservoir, and V is the measurement voltage. Physically, $\Delta I = I_a - I_b$ characterizes the detector's response to the qubit electron's location in the CQDs. The detector is said in the so-called weakly responding regime if $\Delta I \ll I_0 = (I_a + I_b)/2$. In this work we assume this regime, which enables us to ignore the individual electron tunnelling events and treat the current as a continuous diffusive variable.

B. “ n ”-Resolved Master Equation

The so-called “ n ”-resolved master equation is obtained by *partially* tracing out the detector's microscopic degrees of freedom but keeping track of the number “ n ” of electrons that have tunneled through the detector during the time period $(0, t)$ [13, 14, 23]. Originally, it was derived in Ref. 13 from the many-body Schrödinger equation at zero temperature and in the large measurement voltage limit. Later, it was proved that this approach is completely equivalent to the Bayesian approach [15] and the quantum trajectory theory [17], which share the same Lindblad type master equation and its unravelling.

Alternatively, under arbitrary (i.e. not high enough)

voltages, it was found that this measurement problem *cannot* be described by a Lindblad type master equation [22, 23]. In particular, a non-Lindblad type master equation was derived [22], and its “ n ”-resolved counterpart reads [23]

$$\dot{\rho}^{(n)} = -i\mathcal{L}\rho^{(n)} - \frac{1}{2}\{Q\tilde{Q}\rho^{(n)} - \tilde{Q}^{(-)}\rho^{(n-1)}Q - \tilde{Q}^{(+)}\rho^{(n+1)}Q + \text{H.c.}\}. \quad (2)$$

Here, $Q = \mathcal{T} + \chi|a\rangle\langle a|$, $\tilde{Q} = \tilde{Q}^{(+)} + \tilde{Q}^{(-)}$, $\tilde{Q}^{(\pm)} = \tilde{C}^{(\pm)}(\mathcal{L})Q$, and $\tilde{C}^{(\pm)}(\mathcal{L}) = \int_{-\infty}^{\infty} dt C^{(\pm)}(t)e^{-i\mathcal{L}t}$. $C^{(\pm)}(t)$ are the reservoir electron correlation functions. Under wide-band approximation for the QPC reservoirs, the spectral function $\tilde{C}^{(\pm)}(\mathcal{L})$ can be explicitly carried out as $\tilde{C}^{(\pm)}(\mathcal{L}) = 2\pi g_L g_R [x/(1 - e^{-x/T})]_{x=-\mathcal{L}\mp V}$, where T is the reservoir temperature (in this work we use the unit system of $\hbar = e = k_B = 1$). It is of interest to note that the Liouvillian operator \mathcal{L} in $\tilde{C}^{(\pm)}(\mathcal{L})$ contains the information of energy exchange between the detector and the qubit, which correlates the energy relaxation of the measured qubit with the inelastic electron tunnelling in the detector. Note also that in the derivation of the above “ n ”-resolved master equation we did not make assumption of large bias voltage across the QPC detector. At large voltage limit, i.e., the bias voltage is much larger than the internal energy scale of the qubit, the spectral function $\tilde{C}^{(\pm)}(\mathcal{L}) \simeq \tilde{C}^{(\pm)}(0)$, and Eq. (2) reduces to the result obtained in Ref. 13.

Formally, we rewrite Eq. (2) as

$$\dot{\rho}^{(n)} = -i\mathcal{L}\rho^{(n)} - \mathcal{R}\rho^{(n)} + \mathcal{R}_1\rho^{(n-1)} + \mathcal{R}_2\rho^{(n+1)}, \quad (3)$$

where \mathcal{R} , \mathcal{R}_1 and \mathcal{R}_2 are superoperators defined in accord with Eq. (2). To solve this infinite number of coupled equations, we perform the discrete Fourier transformation, $\rho(k, t) = \sum_n e^{ink}\rho^{(n)}(t)$, yielding

$$\dot{\rho}(k, t) = [-i\mathcal{L} - \mathcal{R} + e^{ik}\mathcal{R}_1 + e^{-ik}\mathcal{R}_2]\rho(k, t). \quad (4)$$

Explicitly, in the localized dot-state representation $\{|a\rangle, |b\rangle\}$ we obtain

$$\begin{pmatrix} \dot{\rho}_{aa} \\ \dot{\rho}_{bb} \\ \dot{\rho}_{ab} \\ \dot{\rho}_{ba} \end{pmatrix} = \begin{pmatrix} a_1 & 0 & a_2 + i\Omega & a_2 - i\Omega \\ 0 & b_1 & b_2 - i\Omega & b_2 + i\Omega \\ c_3 + i\Omega & c_2 - i\Omega & c_1 - i\epsilon_a + i\epsilon_b & 0 \\ c_3 - i\Omega & c_2 + i\Omega & 0 & c_1 + i\epsilon_a - i\epsilon_b \end{pmatrix} \begin{pmatrix} \rho_{aa} \\ \rho_{bb} \\ \rho_{ab} \\ \rho_{ba} \end{pmatrix} \quad (5)$$

For brevity, the explicit expressions of the coefficients $a_{1(2)}$, $b_{1(2)}$ and $c_{1(2,3)}$ are ignored here and are put alternatively in Appendix A.

Formally, we reexpress the Fourier-transformed master

equation as $\dot{\rho}(k, t) = \mathcal{M}(k)\rho(k, t)$, and the solution reads $\rho(k, t) = e^{\mathcal{M}(k)(t-t_0)}\rho(k, t_0)$. Note that we are concerned with the “ n ”-resolved state evolution from t_0 to t , i.e., the counting of “ n ” starts from the moment t_0 . We thus

have $\rho^{(n)}(t_0) = \rho(t_0)\delta_{n,0}$, and $\rho(k, t_0) = \rho(t_0)$. With the knowledge of $\rho(k, t)$, the inverse Fourier transform gives

$$\rho^{(n)}(t) = \sum_k e^{-ink} \rho(k, t) = \sum_k e^{-ink} e^{\mathcal{M}(k)(t-t_0)} \rho(t_0). \quad (6)$$

Strikingly, we can introduce a propagator for the state evolution, $\mathcal{U}(n, t) = \sum_k e^{-ink} e^{\mathcal{M}(k)t}$. Since this propagator is completely determined by the *dynamic structure* of the master equation but does not depend on the initial state, we can numerically evaluate it by a ‘‘one-time task’’ via such as the fast Fourier transformation. This feature leads to a very efficient Monte Carlo simulation for the measurement-history conditioned evolution (i.e. the quantum trajectory simulation).

C. Monte Carlo Simulation for Conditional Evolution

It seems that $\rho^{(n)}(t)$ contains *less* information about the measurement record (history) than the conditional state $\rho_c(t)$ in the conventional quantum trajectory theory [17], since it only implies that *totally* there have been n electrons passed through the QPC junction during the specified time period. However, if we make successive readout for the electron numbers ‘‘ n_k ’’ passed through the detector during the time interval (t_{k-1}, t_k) , we actually record the measurement current $I_c(t)$ of a single realization. After each time of reading out ‘‘ n_k ’’, the statistically mixed state $\rho^{(n)}(t_k)$ with any possible ‘‘ n ’’ would ‘‘collapse’’ to a normalized state $\rho^{(n_k)}(t_k)$ with definite ‘‘ $n = n_k$ ’’. The set of records $\{n_k : k = 1, 2, \dots\}$ corresponds to the current $I_c(t)$, and the set of states $\{\rho^{(n_k)}(t_k) : k = 1, 2, \dots\}$ is nothing but the conditional state $\rho_c(t)$ in the quantum trajectory theory.

This *state-update* procedure based on the ‘‘ n ’’-resolved master equation was introduced in Ref. 15, where its exact equivalence to the Bayesian and quantum trajectory theories was analytically proved. That is, the *conditional* master equation can be re-derived based on the ‘‘ n ’’-resolved master equation together with the above ‘‘collapse’’ idea. However, we found that this can be done only in the large voltage limit which leads to a Lindblad-type master equation [15, 17]. For arbitrary voltage, rather than deriving a conditional master equation to describe the measurement-record conditioned evolution, we would like here to develop an efficient numerical unravelling scheme which has the advantage of being applicable to non-Lindblad type master equation as studied in this work.

More quantitatively, let us consider the state evolution during $[t_j, t_j + \tau]$. That is, starting with a definite state at t_j , say $\rho(t_j)$, the state $\rho^{(n_j)}(t_j + \tau)$ at $t_j + \tau$ can be calculated via

$$\rho^{(n_j)}(t_j + \tau) = \mathcal{U}(n_j, \tau)\rho(t_j). \quad (7)$$

If the measurement is made but the result is ignored, the

(mixture) state is described by

$$\rho(t_j + \tau) = \sum_{n_j} \rho^{(n_j)}(t_j + \tau) = \sum_{n_j} \text{Pr}(n_j)\rho_c(n_j, t_j + \tau), \quad (8)$$

where $\text{Pr}(n_j) = \text{Tr}[\rho^{(n_j)}(t_j + \tau)]$ stands for the probability having n_j electrons tunnelled through the detector, and $\rho_c(n_j, t_j + \tau) = \rho^{(n_j)}(t_j + \tau)/\text{Pr}(n_j)$ is the normalized state conditioned by the definite number of n_j electrons observed passed through the detector.

The second equality of Eq.(8) implies that if we stochastically generate n_j according to the probability $\text{Pr}(n_j)$ for each time interval $[t_j, t_j + \tau]$, step by step from t_0 to t , and ‘‘collapse’’ the state definitely onto $\rho_c(n_j, t_j + \tau)$, i.e., $\rho_c(t_j + \tau) = \rho^{(n_j)}(t_j + \tau)/\text{Pr}(n_j) = \mathcal{U}(n_j, \tau)\rho(t_j)/\text{Tr}[\mathcal{U}(n_j, \tau)\rho(t_j)]$, we have in fact simulated a particular realization for the selective state evolution conditioned on the (continuous) specific measurement result. The simple ensemble average over a large number of particular realizations of $\rho_c(t)$ recovers the unconditional state $\rho(t)$. Obviously, this unravelling scheme is completely equivalent to the spirit of the conventional quantum trajectory theory, despite that in this context we are unable to derive an explicit stochastic differential equation to unravel the underlying non-Lindblad master equation. However, they have precisely the same physical meaning.

To stochastically generate n_j according to the probability $\text{Pr}(n_j)$, two procedures are adopted as follows: (i) Based on the ensemble average current $I(t) = \text{Re}\{\text{Tr}[\bar{Q}\rho(t)Q]\}$, which was derived in Ref. 23, the output current in particular measurement realization reads

$$I_c(t) = \text{Re}\{\text{Tr}[\bar{Q}\rho_c(t)Q]\} + \xi(t). \quad (9)$$

The first term in this equation is related to the qubit dynamics of *conditional evolution*. The second noisy term $\xi(t)$ originates from the detector’s *intrinsic* noise, which is a Poissonian variable in the regime of point process, and a Gaussian variable in the diffusive regime. In the latter case, $\xi(t)$ has zero mean value, and the spectral density $S_\xi = 2I_0 \coth \frac{V}{2T}$. At zero temperature and large voltage limit, this treatment recovers the existing result of quantum trajectory theory and Bayesian approach [15, 17], i.e., $I_c(t) = \rho_{c,aa}(t)I_a + \rho_{c,bb}(t)I_b + \xi(t)$, with $S_\xi = 2I_0$. (ii) Straightforwardly, in our simulation we relate the *stochastic* electron number n_j with $I_c(t)$ via $n_j = \int_{t_j}^{t_j+\tau} dt' I_c(t') = \bar{I}_c(t_j)\tau + dW(t_j)$, where $\bar{I}_c(t_j) = \text{Re}\{\text{Tr}[\bar{Q}\rho_c(t_j)Q]\}$, and $dW(t_j)$ is the Wiener increment during $[t_j, t_j + \tau]$.

In Fig. 1 we plot a comparison of the ensemble average of the Monte Carlo simulation (over 500 quantum trajectories) with the result directly given by the unconditional master equation. The excellent agreement shows the validity and efficiency of the proposed unravelling scheme. In this context, two points are likely to be highlighted: (i) the measurement voltage considered here is moderately finite, but not the high voltage limit [15, 17]; (ii) the

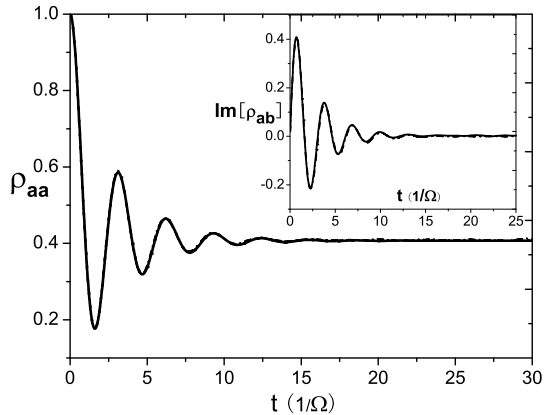


FIG. 1: Ensemble average of the Monte Carlo simulation over 500 quantum trajectories (dash-dotted line) versus the result directly given by the unconditional master equation (solid line). It is assumed that the initial state of the qubit $|\psi\rangle = |a\rangle$. The relevant parameters are: $\mathcal{T} = 20\Omega$, $\chi = 0.7\Omega$, $V = 0.5\Omega$, $\epsilon = 0.25\Omega$, $T = 1.0\Omega$, and $g_{L(R)} = 1/\sqrt{2\pi}\Omega$.

corresponding non-Lindblad master equation is unravelled *physically*, having the same physical interpretation as provided by Wiseman *et al* [6].

In Fig. 2 we show the main features of the conditional state evolution. (i) Assuming that the coherent coupling is switched off ($\Omega = 0$), in Fig. 2(a) we illustrate the wavefunction collapse of a pure state $|\psi\rangle = 1/\sqrt{2}(|a\rangle + |b\rangle)$ under measurement. This feature has deep implication in understanding the *measurement postulate* in quantum mechanics, which has been highlighted by the concept of *gradual collapse* for a typical solid-state two-level state under (weak) measurement, as discussed in particular by Leggett [24]. The reason for this *gradual collapse* is the weak coupling and the finite noise of the detector, which make the quantum measurement need some time until acceptable signal-to-noise ratio is reached. (ii) On the other hand, if $\Omega \neq 0$, the ideal measurement will lead to the *gradual purification* of the qubit state starting, for instance, with a completely mixed state. This is shown by the revival of the coherent Rabi oscillation in Fig. 2(b). (iii) As shown in Fig. 3(c), with the increase of the measurement strength ($|\chi|/\Omega$), the duration time on each qubit state is enhanced, while the switching time between them is reduced. This is an obvious signature of the quantum Zeno effect, appearing in the regime of *gradual* but not the conventional *instantaneous* collapse. (iv) In the conditional dynamics, the output current $I_c(t)$ can basically follow the conditional qubit state, as shown by Fig. 2(d). Due to the intrinsic noise of the detector, here the filtered current, i.e., $\bar{I}_c(t) = \frac{1}{\Delta t} \int_t^{t+\Delta t} I_c(t') dt'$, is plotted, where Δt is the “filtering window”.

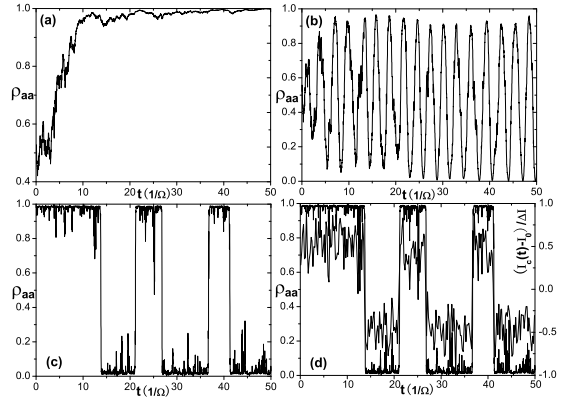


FIG. 2: The main characteristics of the conditional state evolution under continuous measurement: (a) gradual localization ($\Omega = 0$) from an initial superposition state $|\psi\rangle = 1/\sqrt{2}(|a\rangle + |b\rangle)$; (b) gradual purification from a completely mixed state; (c) zeno effect under relatively strong continuous measurement; and (d) conditional state evolution (thick line) versus the filtered output current (thin line), which is obtained by $\frac{1}{\Delta t} \int_t^{t+\Delta t} I_c(t') dt'$, with the filtering window $\Delta t = 0.2/\Omega$. The parameters (\mathcal{T} , χ , V , ϵ , T) are adopted as (in unit of Ω): (a)(20.0, 0.13, 3.0, 0.25, 1.0), (b)(20.0, 0.7, 3.0, 0.25, 1.0), (c)(25.0, 4.0, 3.0, 0.25, 1.0), and (d)(25.0, 4.0, 3.0, 0.25, 1.0). The density of states $g_{L(R)} = 1/\sqrt{2\pi}\Omega$.

D. Noise Spectrum

In the same spirit of conventional quantum trajectory theory [6, 17], the present unravelling scheme also provides a natural way to calculate the output power spectrum. The details of derivation is referred to Appendix B, here we simply present the resultant expression of the output current correlator, which reads

$$\begin{aligned} K_I(\tau) &\equiv E[I_c(t+\tau)I_c(t)] - E[I_c(t+\tau)]E[I_c(t)] \\ &= \text{Tr}[\bar{\mathcal{U}}e^{\mathcal{L}\tau}\bar{\mathcal{U}}\rho(t)] - \text{Tr}[\bar{\mathcal{U}}\rho(t+\tau)]\text{Tr}[\bar{\mathcal{U}}\rho(t)] \\ &\quad + \text{Tr}[\bar{\mathcal{U}}\rho(t)]\delta(\tau), \end{aligned} \quad (10)$$

where $\bar{\mathcal{U}} = \sum_n n\mathcal{U}(n, dt)/dt$, $\bar{\mathcal{U}}' = \sum_n n^2\mathcal{U}(n, dt)/dt$, $\rho(t+\tau) = e^{\mathcal{L}\tau}\rho(t)$. For stationary state $K_I(\tau) = \text{Tr}[\bar{\mathcal{U}}e^{\mathcal{L}\tau}\bar{\mathcal{U}}\rho(\infty)] - \text{Tr}[\bar{\mathcal{U}}\rho(\infty)]^2 + \text{Tr}[\bar{\mathcal{U}}'\rho(\infty)]\delta(\tau)$.

In practice, particularly in the presence of quantum feedback, the ensemble averaged evolution represented by $e^{\mathcal{L}\tau}$ can be implemented by numerically averaging the stochastic trajectories. In the absence of quantum feedback, the above quantum trajectory approach can precisely recover the analytic result of stationary state noise spectrum, obtained by using the MacDonald formula [23].

III. QUANTUM FEEDBACK CONTROL

Quantum feedback control is one of the typical means of quantum coherence control. In quantum optics, the

study of quantum feedback control has been going on for more than a decade [25]. However, it is a relatively new subject in solid states [18, 19, 20]. In particular, the conditional state evolution under continuous weak measurement has been *experimentally* demonstrated in solid-state qubit very recently [26]. This may pave a way to the quantum feedback control in solid-states. For the solid-state setup under present study, we now consider the feedback control of the qubit coherent evolution, by unravelling the underlying measurement dynamics that is in general governed by non-Lindblad master equation.

The basic idea is to convert the measurement information in the output current $I_c(t)$ into the evolution of qubit state $\rho_c(t)$. By comparing $\rho_c(t)$ with the desired state $\rho_d(t)$, their difference is then employed to modify the qubit Hamiltonian in order to reduce their difference in next step evolution. Specifically, we consider a symmetric qubit (i.e. $\epsilon = 0$). The desired state is $|\psi_d(t)\rangle = \cos(\Omega t)|a\rangle - i \sin(\Omega t)|b\rangle$. In real-time feedback control, each successive feedback acts only for an infinitesimal time interval Δt . In the so-called Bayesian state-estimate-based feedback, the suboptimal algorithm is desirable [27, 28]. That is, the algorithm is constructed such that the state evolution in each infinitesimal time step will maximize the fidelity of the estimated state with the desired (target) state. In more detail, as far as the term related to the feedback Hamiltonian is concerned, the state $\rho_c(t + \Delta t)$ is given by

$$\begin{aligned} \rho_c(t + \Delta t) = & \rho_c(t) - i[H_{fb}, \rho_c(t)]\Delta t \\ & - \frac{1}{2}[H_{fb}, [H_{fb}, \rho_c(t)]](\Delta t)^2 + \dots \end{aligned} \quad (11)$$

The fidelity of this state with the target state reads

$$\begin{aligned} & \langle \psi_d(t) | \rho_c(t + \Delta t) | \psi_d(t) \rangle \\ & = \langle \psi_d(t) | \rho_c(t) | \psi_d(t) \rangle - i \langle \psi_d(t) | [H_{fb}, \rho_c(t)] | \psi_d(t) \rangle \Delta t \\ & - \frac{1}{2} \langle \psi_d(t) | [H_{fb}, [H_{fb}, \rho_c(t)]] | \psi_d(t) \rangle (\Delta t)^2 + \dots \end{aligned} \quad (12)$$

To optimize the fidelity, one should maximize the coefficient of Δt , which is the dominant term. Similar to other control theories, the maximization must be subject to certain constraints, e.g., the restriction on the maximum eigenvalue of H_{fb} , the sum of the norms of the eigenvalues, or the sum of the squares of the eigenvalues, etc. Physically, these constraints stem from the limitation of the feedback strength or finite Hamiltonian resources. Here we adopt the last type of constraint, namely, $\text{Tr}[H_{fb}^2] \leq \mu$. Under this constraint, the feedback Hamiltonian can be constructed in terms of

$$H_{fb} = i\lambda[|\psi_d(t)\rangle\langle\psi_d(t)|, \rho_c(t)], \quad (13)$$

where $\lambda = \sqrt{\frac{\mu}{2(a-b^2)}}$, with $a = \langle \psi_d(t) | \rho_c(t) | \psi_d(t) \rangle$, and $b = \langle \psi_d(t) | \rho_c(t) | \psi_d(t) \rangle$.

Combining the above feedback Hamiltonian with the previously developed state unravelling scheme, the estimated state $\rho_c(t)$ can be straightforwardly calculated,

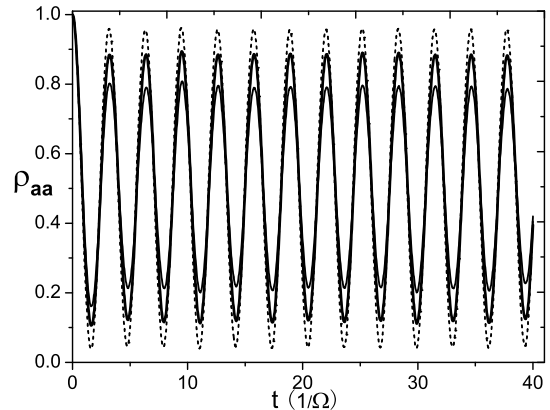


FIG. 3: Feedback control of the coherent oscillation of qubit state, resulting from feedback strengths $\lambda = 0.5$ (thin solid line), 1.0 (thick solid line), and 3.5 (dashed line). The parameters are: $\mathcal{T} = 20.0\Omega$, $\underline{\chi} = 0.7\Omega$, $V = 3.0\Omega$, $\epsilon = 0.0\Omega$, $T = 1.0\Omega$, and $g_{L(R)} = 1/\sqrt{2\pi}\Omega$.

leading to the state propagation in the presence of feedback. Figure 3 shows the control result with quantum feedback, where the ensemble-average has been made over large number of Monte-Carlo simulated trajectories. Here the measurement voltage is quite moderate, i.e., $V = 3\Omega$, which is beyond the theoretical description in large-voltage limit as previously studied [13, 15, 17, 18, 19, 20]. We observe that the control effect is evident: by increasing the feedback strength λ the measurement induced back-action can be largely eliminated, and the desired coherent oscillation of the qubit can be maintained *for arbitrarily long time*.

It will be of interest to compare the quantum measurement in the presence of feedback to the well-known quantum non-demolition (QND) measurement. For the solid-state qubit, elegant schemes of QND measurement have been proposed very recently [29, 30]. Here, for the qubit measurement under consideration, we demonstrate that the QND measurement is equivalent to the usual back-action-present measurement plus quantum feedback. In Fig. 4 we present the calculated output power spectrum of the QPC detector. The peak at $\omega = \Omega$ indicates the coherent oscillation of the qubit. In the absence of feedback, it has been shown that the peak-to-background ratio cannot be larger than 4 [16], due to the back-action of measurement. In the presence of feedback, however, we obtain very sharp peak here which indicates almost ideal coherent oscillations. Theoretically, since no steady-state is available in the presence of feedback, the start time of the qubit evolution is chosen as the *initial time* of the current correlation function, and the noise spectrum is the Fourier transform of the correlate function with respect to the later time (difference). Experimentally, this feedback-induced sharper peak can be employed as an in-

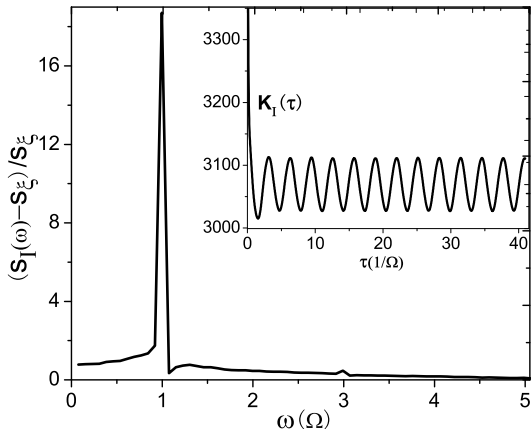


FIG. 4: Narrowed coherence peak in the noise spectrum as an indicator for the feedback effect (Inset: the coherently oscillating correlation function). The parameters are : $\mathcal{T} = 10.0\Omega$, $\chi = 0.2\Omega$, $V = 3.0\Omega$, $\epsilon = 0.0\Omega$, $T = 0.5\Omega$, $\lambda = 15$, and $g_{L(R)} = 1/\sqrt{2\pi}\Omega$.

indicator for the feedback effect in practice. We expect that this kind of experiment can be performed in the not-far future.

Finally, we address the effect of measurement voltage. Figure 5 shows the synchronization degree of the feedback versus the measurement voltage. It is of interest to notice that there exists an *optimal* measurement voltage for relatively small feedback strength. This is because for larger voltage the back-action is relatively too strong, while for smaller voltage the information of the measured state cannot be extracted out efficiently. As a result, the turnover behavior of the synchronization degree versus voltage is found. However, with the increase of the feedback strength, the strong back-action can be eliminated more efficiently by the feedback. In this case, the synchronization degree does not decrease considerably as the measurement voltage increases, as shown in Fig. 5.

IV. CONCLUDING REMARKS

To summarize, in the context of continuous quantum measurement and coherence control of solid-state charge qubit, we have presented an unravelling scheme for the non-Lindblad type master equation. Based on it, we also constructed an efficient method to calculate the noise spectrum, which can be regarded as a generalization of the standard quantum jump theory developed in quantum optics. Despite the absence of analytic formalism, the numerical implementation in practice was demonstrated to be straightforward and efficient. Illustrative application was further contributed to the quantum feedback control under arbitrary measurement volt-

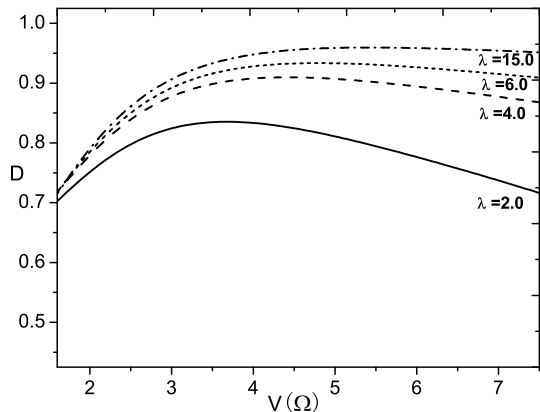


FIG. 5: Effect of measurement voltage on the feedback control. Here the quantity *synchronization degree*, which is defined as $D = 2\langle \text{Tr}[\rho_c(t)\rho_d(t)] \rangle - 1$, with $\langle \dots \rangle$ meaning the average over time, is employed to characterize the control quality. Note that for perfect control the synchronization degree is unity (i.e., $D = 1$). The parameters are: $\mathcal{T} = 20.0\Omega$, $\chi = 0.7\Omega$, $\epsilon = 0.0\Omega$, $T = 1.0\Omega$, and $g_{L(R)} = 1/\sqrt{2\pi}\Omega$.

ages. The detector noise spectrum under feedback was calculated, and its narrowing clearly reflected the control effect. Also, the effect of measurement voltage was discussed.

The present study has been focused on the setup of double-dot qubit measured by quantum point contact. However, for other solid-state setup such as charge qubit measured by single-electron-transistor, similar unravelling scheme can be constructed. Owing to the fact that in general (e.g. in the presence of many-body Coulomb correlations) the measurement dynamics is not governed by Lindblad type master equation, the present “n”-resolved master equation based unravelling scheme seems quite desirable. Finally, in spite of the various unravelling schemes for non-Lindblad type master equation or even for non-Markovian dissipative systems, to our knowledge all of them are largely *mathematical*. Therefore, the present *physical* unravelling scheme is of interest and valuable, which may find applications in the field of solid-state quantum information.

Acknowledgments. Support from the National Natural Science Foundation of China (No. 90203014, 60376037, and 60425412), the Major State Basic Research Project No. G001CB3095 of China, and the Research Grants Council of the Hong Kong Government is gratefully acknowledged.

APPENDIX A: MATRIX ELEMENTS OF $\mathcal{M}(k)$

The coefficients in Eq.(5) read

$$a_1 = -Q_{aa}[\tilde{Q}_{aa} - e^{ik}\tilde{Q}_{aa}^{(-)} - e^{-ik}\tilde{Q}_{aa}^{(+)}], \quad (\text{A1a})$$

$$a_2 = -\frac{Q_{aa}}{2}[\tilde{Q}_{ab} - e^{ik}\tilde{Q}_{ab}^{(-)} - e^{-ik}\tilde{Q}_{ab}^{(+)}], \quad (\text{A1b})$$

$$b_1 = -Q_{bb}[\tilde{Q}_{bb} - e^{ik}\tilde{Q}_{bb}^{(-)} - e^{-ik}\tilde{Q}_{bb}^{(+)}], \quad (\text{A1c})$$

$$b_2 = -\frac{Q_{bb}}{2}[\tilde{Q}_{ba} - e^{ik}\tilde{Q}_{ba}^{(-)} - e^{-ik}\tilde{Q}_{ba}^{(+)}], \quad (\text{A1d})$$

$$c_1 = -\frac{1}{2}[(Q_{aa}\tilde{Q}_{aa} + Q_{bb}\tilde{Q}_{bb}) - e^{ik}(Q_{aa}\tilde{Q}_{bb}^{(-)} + Q_{bb}\tilde{Q}_{aa}^{(-)}) - e^{-ik}(Q_{aa}\tilde{Q}_{bb}^{(+)} + Q_{bb}\tilde{Q}_{aa}^{(+)}), \quad (\text{A1e})$$

$$c_2 = -\frac{1}{2}[Q_{aa}\tilde{Q}_{ab} - e^{ik}Q_{bb}\tilde{Q}_{ab}^{(-)} - e^{-ik}Q_{bb}\tilde{Q}_{ab}^{(+)}], \quad (\text{A1f})$$

$$c_3 = -\frac{1}{2}[Q_{bb}\tilde{Q}_{ba} - e^{ik}Q_{aa}\tilde{Q}_{ba}^{(-)} - e^{-ik}Q_{aa}\tilde{Q}_{ba}^{(+)}], \quad (\text{A1g})$$

where

$$\tilde{Q}_{aa}^{(\pm)} = \tilde{C}^{(\pm)}(0)[T + \frac{1}{2}\chi(1 + \cos^2\theta)] + \chi\lambda_{\pm}\sin^2\theta,$$

$$\tilde{Q}_{bb}^{(\pm)} = \tilde{C}^{(\pm)}(0)[T + \frac{1}{2}\chi(1 + \sin^2\theta)] - \chi\lambda_{\pm}\sin^2\theta,$$

$$\tilde{Q}_{ab}^{(\pm)} = \frac{1}{2}\chi\tilde{C}^{(\pm)}(0)\sin\theta\cos\theta + \chi\sin\theta(\bar{\lambda}_{\pm} - \lambda_{\pm}\cos\theta),$$

$$\tilde{Q}_{ba}^{(\pm)} = \frac{1}{2}\chi\tilde{C}^{(\pm)}(0)\sin\theta\cos\theta - \chi\sin\theta(\bar{\lambda}_{\pm} + \lambda_{\pm}\cos\theta),$$

$$Q_{aa} = T + \chi, Q_{bb} = T, Q_{ab} = Q_{ba} = 0,$$

and

$$\lambda_{\pm} = \frac{1}{4}[\tilde{C}^{(\pm)}(-\Delta) + \tilde{C}^{(\pm)}(\Delta)],$$

$$\bar{\lambda}_{\pm} = \frac{1}{4}[\tilde{C}^{(\pm)}(-\Delta) - \tilde{C}^{(\pm)}(\Delta)].$$

APPENDIX B: NOISE SPECTRUM

In this appendix, along the line of the conventional quantum jump theory, we extend the method of noise spectrum calculation to the unravelling approach developed in this work. Consider the correlation function $E[dn(t + \tau)dn(t)]$, where $E[dn(t)] = \sum_{n_1} n_1 \text{Tr}[\mathcal{U}(n_1, dt)\rho(t)]$. First, for the case $\tau > 0$,

$$\begin{aligned} E[dn(t + \tau)dn(t)] &= \sum_{n_1} n_1 \text{Prob}[dn(t) = n_1] E[dn_c(t + \tau)|_{dn(t)=n_1}], \quad (\text{B1}) \end{aligned}$$

where $\text{Prob}[dn(t) = n_1] = \text{Tr}[\mathcal{U}(n_1, dt)\rho(t)]$. At time $t + dt$ a definite value n_1 is picked out and the qubit state undergoes an immediate collapse, i.e. $\rho_c(t + dt) = \mathcal{U}(n_1, dt)\rho(t)/\text{Prob}[dn(t) = n_1]$. During the time period $[t + dt, t + \tau]$, one can ignore the measurement records owing to the ensemble nature of the correlation function, therefore

$$\begin{aligned} E[dn_c(t + \tau)|_{dn(t)=n_1}] &= \sum_{n_2} n_2 \text{Tr}[\mathcal{U}(n_2, dt)e^{\mathcal{L}(\tau-dt)} \frac{\mathcal{U}(n_1, dt)\rho(t)}{\text{Prob}[dn(t) = n_1]}]. \quad (\text{B2}) \end{aligned}$$

To the leading order of dt we have

$$E[dn(t + \tau)dn(t)] = \sum_{n_1 n_2} n_2 \text{Tr}[\mathcal{U}(n_2, dt)e^{\mathcal{L}\tau} \times \frac{\mathcal{U}(n_1, dt)\rho(t)}{\text{Tr}[\mathcal{U}(n_1, dt)\rho(t)]}] n_1 \text{Tr}[\mathcal{U}(n_1, dt)\rho(t)] = \text{Tr}[\bar{\mathcal{U}}e^{\mathcal{L}\tau}\bar{\mathcal{U}}\rho(t)]dt^2. \quad (\text{B3})$$

Here we have introduced $\bar{\mathcal{U}} \equiv \sum_n n\mathcal{U}(n, dt)/dt$. Next for $\tau = 0$ we have

$$\begin{aligned} E[dn(t)^2] &= \sum_n n^2 \text{Prob}[dn(t) = n] \\ &= \sum_n n^2 \text{Tr}[\mathcal{U}(n, dt)\rho(t)] \\ &= \text{Tr}[\bar{\mathcal{U}}'\rho(t)]dt, \quad (\text{B4}) \end{aligned}$$

where $\bar{\mathcal{U}}' = \sum_n n^2\mathcal{U}(n, dt)/dt$. For short time τ this equal-time correlation will be dominant, and $E[\frac{dn(t+\tau)}{dt}\frac{dn(t)}{dt}]$ can be treated as δ -correlated noise for

a suitably defined δ function. We thus obtain

$$\begin{aligned} K_I(\tau) &= E[\frac{dn(t+\tau)}{dt}\frac{dn(t)}{dt}] - E[\frac{dn(t+\tau)}{dt}]E[\frac{dn(t)}{dt}] \\ &= \text{Tr}[\bar{\mathcal{U}}e^{\mathcal{L}\tau}\bar{\mathcal{U}}\rho(t)] - \text{Tr}[\bar{\mathcal{U}}\rho(t + \tau)]\text{Tr}[\bar{\mathcal{U}}\rho(t)] \\ &\quad + \text{Tr}[\bar{\mathcal{U}}'\rho(t)]\delta(\tau). \quad (\text{B5}) \end{aligned}$$

Finally, it should be noted that $[dn(t)]^2 \neq dn(t)$ in our above treatment. This differs from the conventional quantum jump theory where the stochastic number $dn(t) = 0$ or 1 in the point process.

-
- [1] N. Gisin, Phys. Rev. Lett **52**, 1657 (1984)
- [2] P. Zoller M. Marte, D.F. Walls, Phys. Rev. A **35**, 198 (1987)
- [3] N. Gisin I.C. Percival, J. Phys. A **25**, 5677 (1992)
- [4] J. Dalibard Y. Castin K. Molmer, Phys. Rev. Lett **68**, 580 (1992)
- [5] H.J. Carmichael, *An Open System Approach to Quantum Optics*, Lecture Notes in Physics(Springer, Berlin, 1993)
- [6] H.M. Wiseman G.J. Milburn, Phys. Rev. A **47**, 1652 (1993)
- [7] M.B. Plenio P.L. Knight, Rev. Mod. Phys **70**, 101 (1998)
- [8] H-P. Breuer, B. Kappler, and F. Petruccione, Phys. Rev. A **59**, 1633 (1999).
- [9] A. Imamoglu, Phys. Rev. A **50**, 3650, (1994).
- [10] W.T. Strunz, L. Diósi and N. Gisin, Phys. Rev. Lett. **82**, 1801, (1999); W.T. Strunz, L. Diósi, N. Gisin and T. Yu, Phys. Rev. Lett. **83**, 4909, (1999).
- [11] J.T. Stockburger, C.H. Mak, Phys. Rev. Lett. **80**, 2657 (1998); J. Chem. Phys. **110**, 4983 (1999); J.T. Stockburger, H. Grabert, Chem. Phys. **268**, 249 (2001); Phys. Rev. Lett. **88**, 170407 (2002).
- [12] J. Shao, J. Chem. Phys. **120**, 5053 (2004).
- [13] S.A. Gurvitz, Phys. Rev. B **56**, 15215 (1997).
- [14] A. Shnirman and G. Schön, Phys. Rev. B **57**, 15400 (1998); Y. Makhlin, G. Schön, and A. Shnirman, Rev. Mod. Phys. **73**, 357 (2001).
- [15] A.N. Korotkov, Phys. Rev. B **60**, 5737 (1999); *ibid.* **63**, 115403 (2001).
- [16] A.N.Korotkov and D.V.Averin, Phys. Rev. B **64**, 165310 (2001)
- [17] H.S. Goan, G.J. Milburn, H.M. Wiseman, and H.B. Sun, Phys. Rev. B **63**, 125326 (2001)
- [18] R. Ruskov and A. N. Korotkov, Phys. Rev. B **66**, 041401(R) (2002); A. N. Korotkov, Phys. Rev. B **71**, 201305(R) (2005); Q. Zhang, R. Ruskov, and A. N. Korotkov, Phys. Rev. B **72**, 245322 (2005).
- [19] A. Hopkins, K. Jacobs, S. Habib, and K. Schwab, Phys. Rev. B **68**, 235328 (2003).
- [20] R. Ruskov, K. Schwab, and A. N. Korotkov, IEEE Trans. Nanotech. **4**, 132 (1995); Phys. Rev. B **71**, 235407 (2005).
- [21] T. Hayashi et al, Phys. Rev. Lett. **91**, 226804 (2003); J.M. Elzerman et al, Phys. Rev. B **67**, R161308 (2003); J.R. Petta et al, Phys. Rev. Lett. **93**, 186802 (2004).
- [22] Xin-Qi Li, Wen-Kai Zhang, Ping Cui, Jiushu Shao, Zhongshui Ma, and Yijing Yan, Phys. Rev. B **69**, 085315 (2004)
- [23] Xin-Qi Li, Ping Cui, and YiJing Yan, Phys. Rev. Lett. **94**, 066803 (2005)
- [24] A. O. Caldeira and A. J. Leggett, Ann. Phys. (N.Y.) **149**, 374 (1983).
- [25] H.M.Wiseman and G.J.Milburn, Phys. Rev. Lett. **70**, 548 (1993); Phys. Rev. A **47**, 642 (1993); Phys. Rev. A **49**, 4110 (1994).
- [26] N. Katz, M. Ansmann, R.C. Bialczak, E. Lucero, R. McDermott, M. Neeley, M. Steffen, E.M. Weig, A.N. Cleland, J.M. Martinis, and A.N. Korotkov, Science **312**, 1498 (2006).
- [27] A.C.Doherty, K.Jacobs, G.Jungman, Phys. Rev. A **63**, 062306 (2001)
- [28] Jinshuang Jin, Xin-Qi Li, and YiJing Yan, Phys. Rev. B **73**, 233302 (2006)
- [29] D.V.Averin, Phys. Rev. Lett. **88**, 207901 (2002)
- [30] Andrew N. Jordan and Markus Buttiker, Phys. Rev. B **71**, 125333 (2005)